Academic Journal of Engineering and Technology Science
ISSN 2616-5767 Vol. 2, Issue 1: 64-70, DOI: 10.25236/AJETS.020016

Preparation and Photoconductive Properties of WO_3 Nanowires

Bing Yu

Department of Electronic Engineering, Jinan University, Guangzhou, Guangdong, 510632, PR China
ybing94@stu2016.jnu.edu.cn

ABSTRACT. *According to the principle of PVD (Physical Vapor Deposition), a large number of WO_3 nanowires having a flat surface and a thickness of 60nm were obtained by a simple one-step method. We characterized the material properties and photoconductivity of WO_3 nanowires by AFM, TEM, Raman spectra and found it has a good photoresponse to the illumination of 405nm light.*

KEYWORDS: *Tungsten oxide, Physical Vapor Deposition, Photoconductive*

1. Introduction

In the development of low-dimensional nanomaterials, nanowires have attracted the attention of researchers due to their unique anisotropy[1]. Transition metal oxides have received widespread attention because of their special physical and chemical properties. Since the transition metal has a d shell, the difference in electron shells filled or not makes the transition metal oxide have a large difference in physical and chemical properties. The properties of transition metal oxides cover almost all aspects of physics and materials science, including superconductivity, semiconductivity, magnetism and ferroelectricity.[2][3][4] Transition metal oxides often have a non-stoichiometric ratio, and oxides having such structural properties are also called functional oxides. In order to improve its electrical, optical and magnetic properties, its structural properties can be adjusted to make it play a greater role in the fields of sensing, electronics and biology. [5][6][7]

Tungsten oxide is an important wide band gap semiconductor material and has received much attention in recent years. Tungsten oxide with many different stoichiometric ratios also exhibits a wide variety of physical and chemical properties. Tungsten oxide with many different stoichiometric ratios also exhibits a wide variety of physical and chemical properties.[8] Some common tungsten oxides are WO_2, $WO_{2.72}$, $WO_{2.9}$, WO_3, etc.[9] Tungsten trioxide (WO_3) with a 2.5~3.5eV band gap has wide application prospects in the field of flat panel displays[10], smart window[11][12], sensor[13], catalyst[14][15] due to its rich characteristics.

Besides, its rich earth content, adjustable height of components, high chemical stability at low pH, and excellent electrical conductivity make it an oxide material that is very promising in the energy field.

In order to grow WO_3 nanomaterials, a common method is to use CVD (Chemical Vapor Deposition), use tungsten carbonyl[16] or needle-shaped tungsten[17] as the source material. In addition to this, there is a sol-gel method[18][19]. We describe a simple method for preparing WO_3 nanowires in this paper. Using tungsten trioxide powder as a source, the PVD principle is applied, and nanowires with good surface morphology are obtained by controlling the heating temperature and the carrier gas. The composition of the obtained material was then verified by Raman spectroscopy. The surface of the nanowires was observed by AFM (Atomic Force Microscope) and TEM (Transmission Electron Microscope), and the photoconductive properties were also characterized.

2. Experimental

The equipment we use is a horizontal tube furnace. The required source material is tungsten trioxide powder [aladdin, <200nm, 99.9%>], and the tungsten trioxide powder is evenly spread on the bottom of the crucible and placed at the center of the quartz tube. The washed silica was placed as a substrate for the growth of the tungsten trioxide nanowires on the side of the crucible from the carrier gas. I tried different carrier gases: Ar and O_2, and the best nanowires growth conditions were obtained by placing 0.02 g WO_3 powder in a tube furnace, setting the carrier gas Ar flow rate to 60 sccm, and heating from room temperature to 30°C/min. The temperature is naturally lowered after 30 minutes at 900 °C. Photodetectors are fabricated by masking and vacuum thermal evaporation processes.

Further, in order to observe the surface morphology of the grown nanowires, we use AFM and TEM characterization techniques.

3. Results & Discussion

Fig.1 shows a 200x optical picture of nanowires grown at different Ar flows. Obviously the nanowires obtained at 60 sccm are optimally sized and the substrate surface is cleaner. Sample (c) was selected for AFM and TEM characterization, as shown in Fig.2(a)(b)(c), the surface of the nanowire was flat, with a width of about 5 μm and a thickness of about 60 nm, indicating~80 layers of WO_3 (single layer of WO_3 has a thickness of about 7.6Å). For the same nanowires, the color of the nanowires is different. It can be seen that the nanowires are distorted during the growth process in the TEM image, and the different thicknesses make the nanowires have different shades of color.

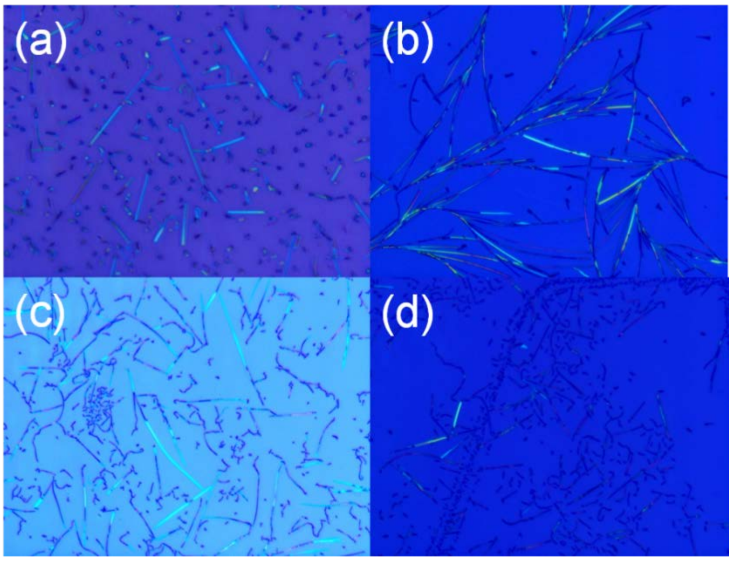

Figure. 1 WO_3 nanowires grown when the Ar flow rate is (a)20 sccm(b)40 sccm(c)60 sccm(d)80 sccm.

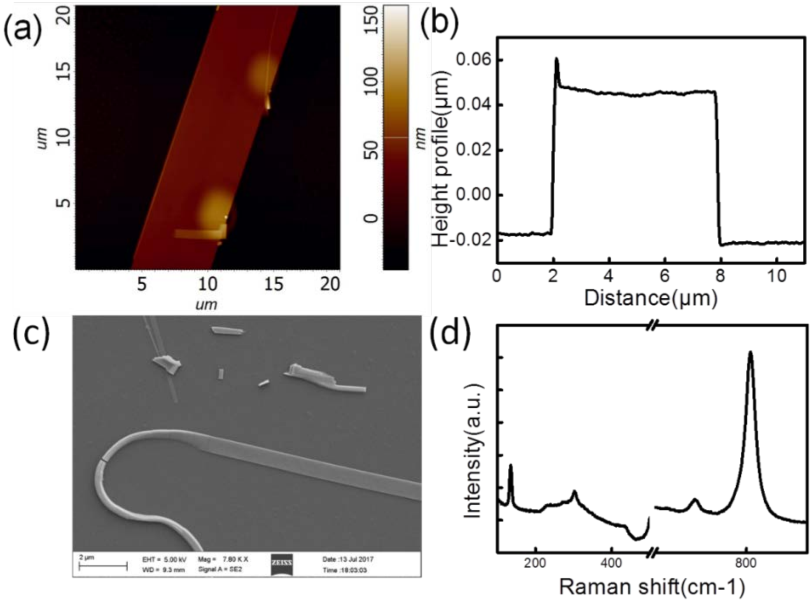

Figure. 2 (a)AFM image, (b)Height profile, (c)TEM image, (d) Raman spectrum of WO_3 nanowires obtained when the Ar flow rate was 60 sccm.

We used Raman spectra to characterize whether the nanowires grown on the silica are WO_3. Raman spectroscopy is a method that does not destroy the surface characteristics of nanometer materials. It has the advantages of rich information acquisition, simple sample preparation method and little influence by water. Fig.2 (d) shows that there are several obvious peaks, of which $135CM^{-1}$, $273CM^{-1}$ corresponds to W-O-W bending mode, and $715cm^{-1}$, $807cm^{-1}$ corresponds to W-O-W stretch mode, which is consistent with the data reported previously[20].

Fig.3 shows the structure of the photoconductive detector. A 104.6 μm length channel was reserved on a WO_3 nanowire grown on SiO_2, and an Au electrode was fabricated on both ends of the nanowire by vacuum thermal evaporation. A visible light with a wavelength of 405nm was selected to be vertically irradiated on the device, and the work current of the device changed with the switching of the light. Theoretically, the photon energy of light at 405nm wavelength is greater than the forbidden band width of WO_3, and the device performs correspondingly to the illumination.

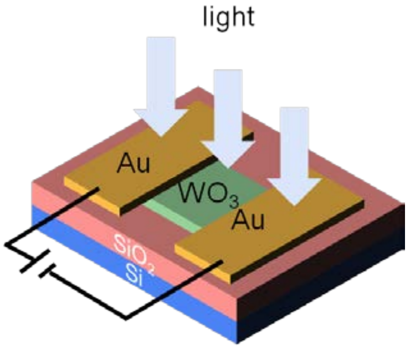

Figure. 3 Schematic of the device.

The photocurrent curve of the WO_3 photoconductive detector is shown in the Fig.3 under different intensities of 405nm light in vacuum. The peak value of the current is positively correlated with the power of the light. The parameters for measuring the photoconductivity response of a material include spectral responsivity (R_λ) and external quantum efficiency (EQE), where R_λ represents the photocurrent generated per unit of power incident light on the active area of the optical device, and EQE represents the number of electron-hole pairs per unit time that can be excited by an adsorbed photon. Respectively expressed by the following equation:

$$R_\lambda = \frac{\triangle I_\lambda}{P_\lambda \cdot S}$$

$$EQE = hcR_\lambda/(e\lambda)$$

Where $\triangle I_\lambda = I_\lambda - I_{dark}$ represents the difference between photocurrent and dark current, P_λ indicates the light intensity per unit area, S is the effective illuminated area, h is Planck's constant (6.63×10-34J·s), c is the velocity of light (3×10^8m/s), λ is the wavelength of incident light.

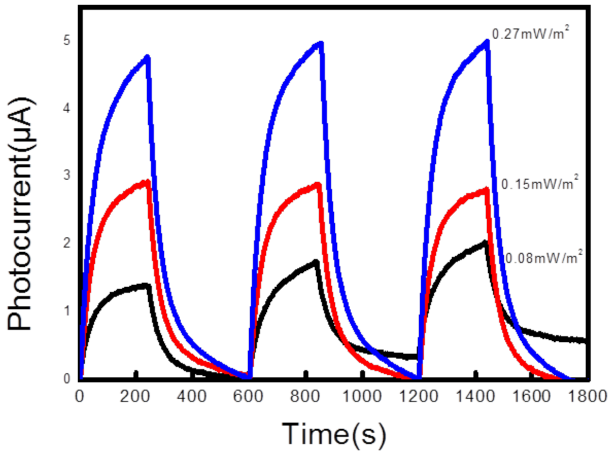

Figure. 4 The photocurrent-time curve with the change of light intensity.

Table 1 Comparison of photoresponse parameters of WO_3 nanowires under different light intensity

Wavelength	S	P_λ	$\triangle I_\lambda$	R_λ	EQE
405nm	4.7×10^{-9}cm^2	0.08W/m^2	1.6μA	0.043	0.132
		0.15mW/m^2	2.85μA	0.040	0.123
		0.27mW/m^2	4.94μA	0.040	0.123

As shown in Table 1, in the photoconductive detector, R_λ and EQE can be estimated to be about 0.041A/W and 12.6 %.

4. Conclusion

In summary, massive WO_3 nanowires were successfully fabricated by one-step PVD method, and its photoconductivity was verified by illumination at 405nm. The values of R_λ and EQE are 0.041A/W and 12.6 %, respectively. The obtained WO_3 nanowires have reversible and stable photoelectric properties and have the potential to be fabricated into photodetectors.

References

[1] Devan, R. S., Patil, R. A., Lin, J. H., & Ma, Y. R. (2012). One-dimensional metal-oxide nanostructures: recent developments in synthesis, characterization, and applications. Advanced Functional Materials, 22 (16), 3326-3370.
[2] Shrotriya, V., Li, G., Yao, Y., Chu, C. W., & Yang, Y. (2006). Transition metal oxides as the buffer layer for polymer photovoltaic cells. Applied Physics Letters, 88 (7), 073508.
[3] Poizot, P. L. S. G., Laruelle, S., Grugeon, S., Dupont, L., & Tarascon, J. M. (2000). Nano-sized transition-metal oxides as negative-electrode materials for lithium-ion batteries. Nature, 407 (6803), 496.
[4] Sawa, A. (2008). Resistive switching in transition metal oxides. Materials today, 11 (6), 28-36.
[5] Yuhas, B. D., Zitoun, D. O., Pauzauskie, P. J., He, R., & Yang, P. (2006). Transition-metal doped zinc oxide nanowires. Angewandte Chemie, 118 (3), 434-437.
[6] Peng, Z., Jiang, W., & Liu, H. (2007). Synthesis and electrical properties of tungsten-doped vanadium dioxide nanopowders by thermolysis. The Journal of Physical Chemistry C, 111 (3), 1119-1122.
[7] Jeong, Y. G., Han, S., Rhie, J., Kyoung, J. S., Choi, J. W., Park, N., ... & Kim, D. S. (2015). A vanadium dioxide metamaterial disengaged from insulator-to-metal transition. Nano letters, 15 (10), 6318-6323.
[8] Huang, Z. F., Song, J., Pan, L., Zhang, X., Wang, L., & Zou, J. J. (2015). Tungsten oxides for photocatalysis, electrochemistry, and phototherapy. Advanced Materials, 27 (36), 5309-5327.
[9] Devan, R. S., Patil, R. A., Lin, J. H., & Ma, Y. R. (2012). One-dimensional metal-oxide nanostructures: recent developments in synthesis, characterization, and applications. Advanced Functional Materials, 22 (16), 3326-3370.
[10] Gavrilyuk, A. I. (1999). Photochromism in WO3 thin films. Electrochimica Acta, 44 (18), 3027-3037.
[11] Li, H., Lv, Y., Zhang, X., Wang, X., & Liu, X. (2015). High-performance ITO-free electrochromic films based on bi-functional stacked WO3/Ag/WO3 structures. Solar Energy Materials and Solar Cells, 136, 86-91.
[12] Chang-Jian, C. W., Cho, E. C., Yen, S. C., Ho, B. C., Lee, K. C., Huang, J. H., & Hsiao, Y. S. (2018). Facile preparation of WO3/PEDOT: PSS composite for inkjet printed electrochromic window and its performance for heat shielding. Dyes and Pigments, 148, 465-473.
[13] Eranna, G. (2016). Metal oxide nanostructures as gas sensing devices. CRC Press.
[14] Kim, S. J., Choi, S. J., Jang, J. S., Kim, N. H., Hakim, M., Tuller, H. L., & Kim, I. D. (2016). Mesoporous WO3 nanofibers with protein-templated nanoscale catalysts for detection of trace biomarkers in exhaled breath. ACS nano, 10 (6), 5891-5899.
[15] Xue, Q., Liu, Y., Zhou, Q., Utsumi, M., Zhang, Z., & Sugiura, N. (2016). Photocatalytic degradation of geosmin by Pd nanoparticle modified WO3 catalyst under simulated solar light. Chemical Engineering Journal, 283, 614-621.

[16] Maruyama, T., & Arai, S. (1994). Electrochromic properties of tungsten trioxide thin films prepared by chemical vapor deposition. *Journal of the Electrochemical Society*, *141* (4), 1021-1024.

[17] Vaddiraju, S., Chandrasekaran, H., & Sunkara, M. K. (2003). Vapor phase synthesis of tungsten nanowires. Journal of the American Chemical Society, 125 (36), 10792-10793.

[18] Badilescu, S., & Ashrit, P. V. (2003). Study of sol–gel prepared nanostructured WO3 thin films and composites for electrochromic applications. Solid State Ionics, 158 (1-2), 187-197.

[19] Luo, Z., Yang, J., Cai, H., Li, H., Ren, X., Liu, J., & Liang, X. (2008). Preparation of silane-WO3 film through sol–gel method and characterization of photochromism. Thin Solid Films, 516 (16), 5541-5544.

[20] Lu, D. Y., Chen, J., Chen, H. J., Gong, L., Deng, S. Z., Xu, N. S., & Liu, Y. L. (2007). Raman study of thermochromic phase transition in tungsten trioxide nanowires. *Applied physics letters*, *90* (4), 041919.